Supplementary Materials

Resolution of Chiral polyoxoanion $[P_2Mo_{18}O_{62}]^{6-}$ with Histidine

Ding Liu, Hua-Qiao Tan, Wei-Lin Chen, Yang-Guang Li,* En-Bo Wang*

Key Laboratory of Polyoxometalate Science of Ministry of Education, Department of Chemistry, Northeast Normal University, Ren Min Street No.5268, Changchun, Jilin 130024, P. R. China.

*To whom correspondence should be addressed. E-mail: wangeb889@nenu.edu.cn, liyg658@nenu.edu.cn. Fax: +86- 431-85098787.

General methods and materials:

All chemicals were commercially purchased and used without further purification. Elemental analyses (C, H, N) were performed on a Perkin-Elmer 2400 CHN elemental analyzer; P, Mo were analyzed on a PLASMA-SPEC(I) ICP atomic emission spectrometer. IR spectra were recorded in the range of 400 ~ 4000 cm^{-1} on an Alpha Centaurt FT/IR Spectrophotometer using KBr pellets. The UV-vis absorption spectra were recorded using a Hitachi UV-3010 spectrophotometer. TG analysis was performed on a Perkin-Elmer TGA7 instrument in flowing N_2 with a heating rate of 10 ºC min^{-1}. Solid-state CD spectra for compounds **1** were recorded using a JASCO J-810 spectrophotometer. Polarizing optical microscope measurements were performed using a Changfang XPV-400E polarized optical microscope.

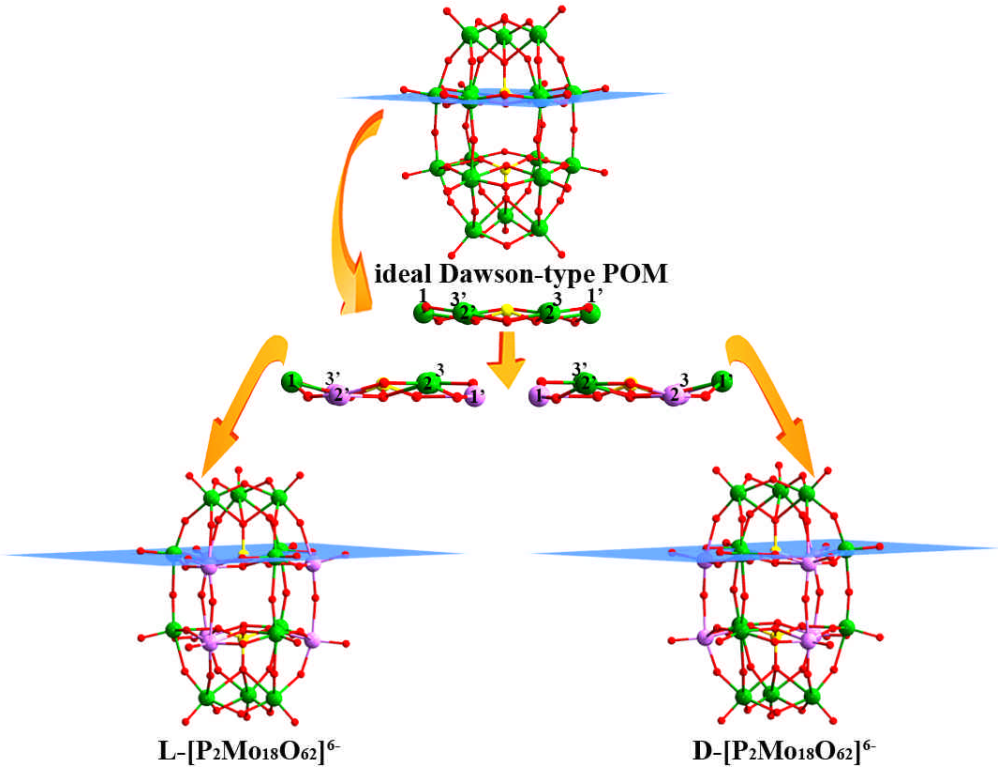

Scheme S1 The L-$[P_2Mo_{18}O_{62}]^{6-}$ and D-$[P_2Mo_{18}O_{62}]^{6-}$ with D_3 symmetry viewed as a ideal Dawson-type polyoxoanion by displacing two different sets of three Mo atoms in the ring.

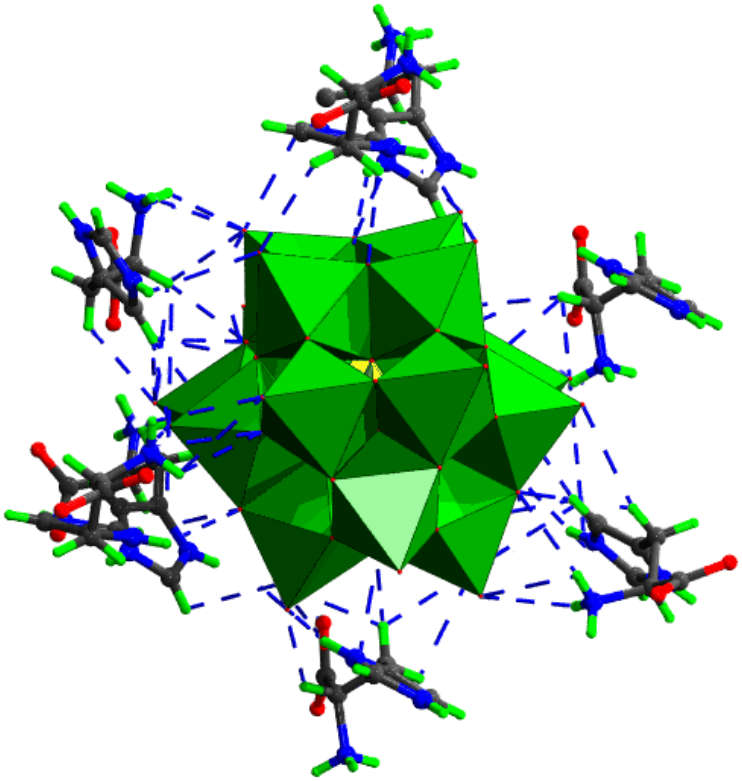

Figure S1 Polyhedral and ball-and-stick representation of the H-bonding interactions between the $[P_2Mo_{18}O_{62}]^{6-}$ polyoxoanions and histidine molecules in compound **1a**.

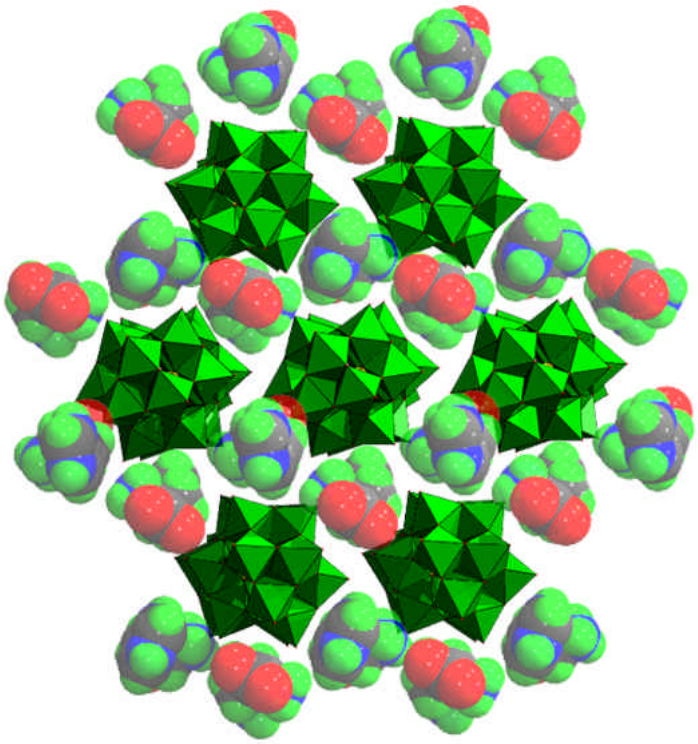

Figure S2 Polyhedral and filling diagram representation of the 2D layer formed of $[P_2Mo_{18}O_{62}]^{6-}$ polyoxoanion and L-histidine in compound **1a.**

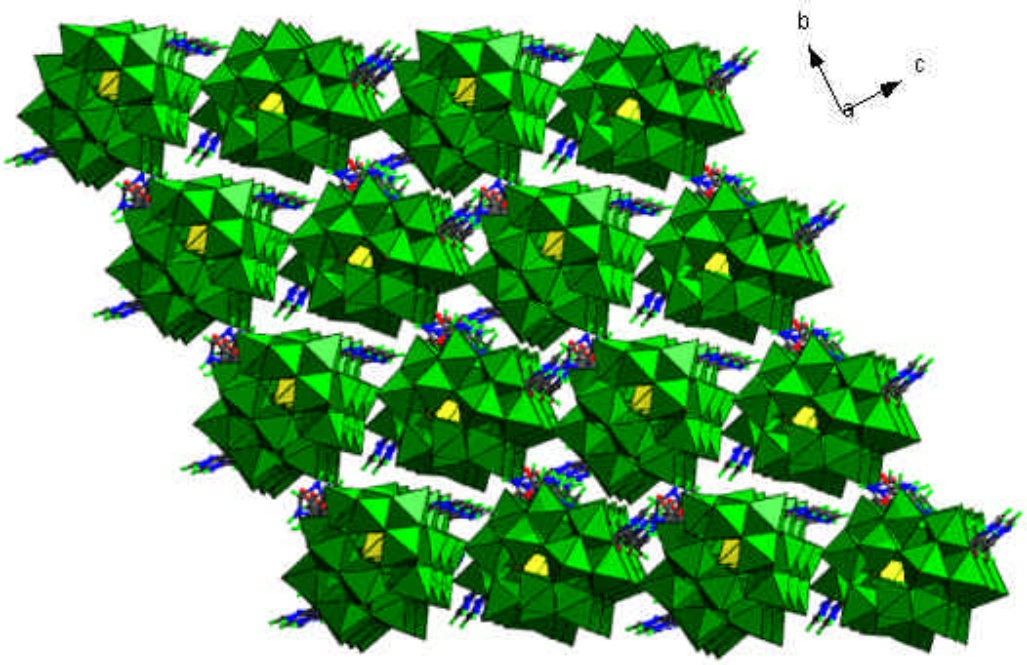

Figure S3 Polyhedral and ball-and-stick representation of the 3D supramolecular structure of **1a** viewed along a axis

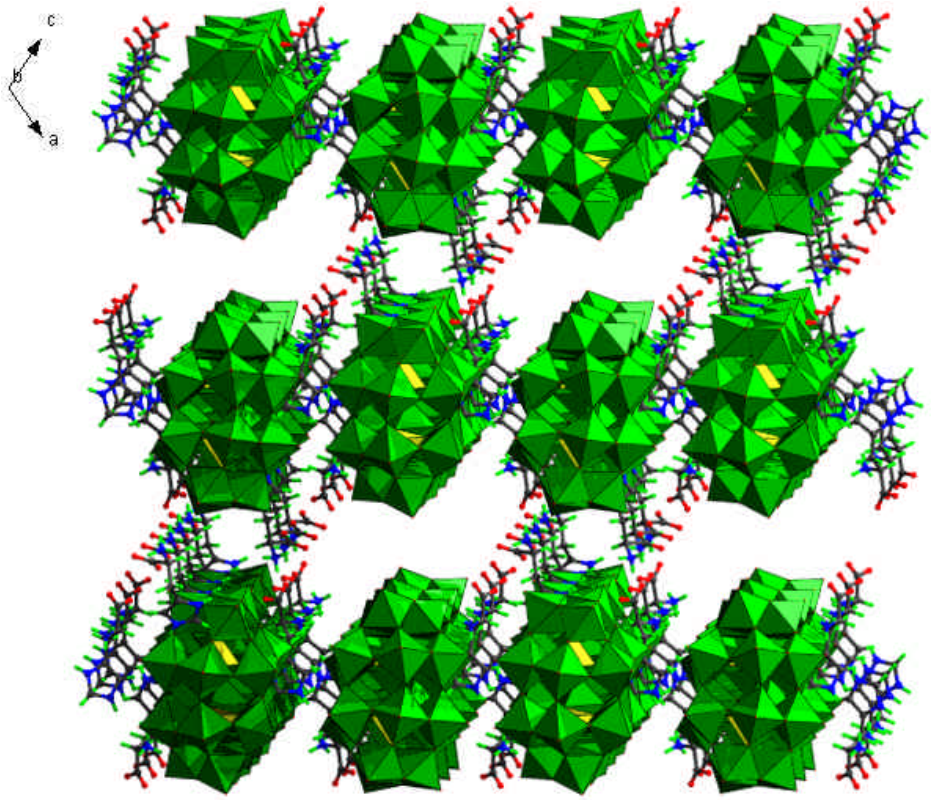

Figure S4 Polyhedral and ball-and-stick representation of the 3D supramolecular structure of **1a** viewed along b axis

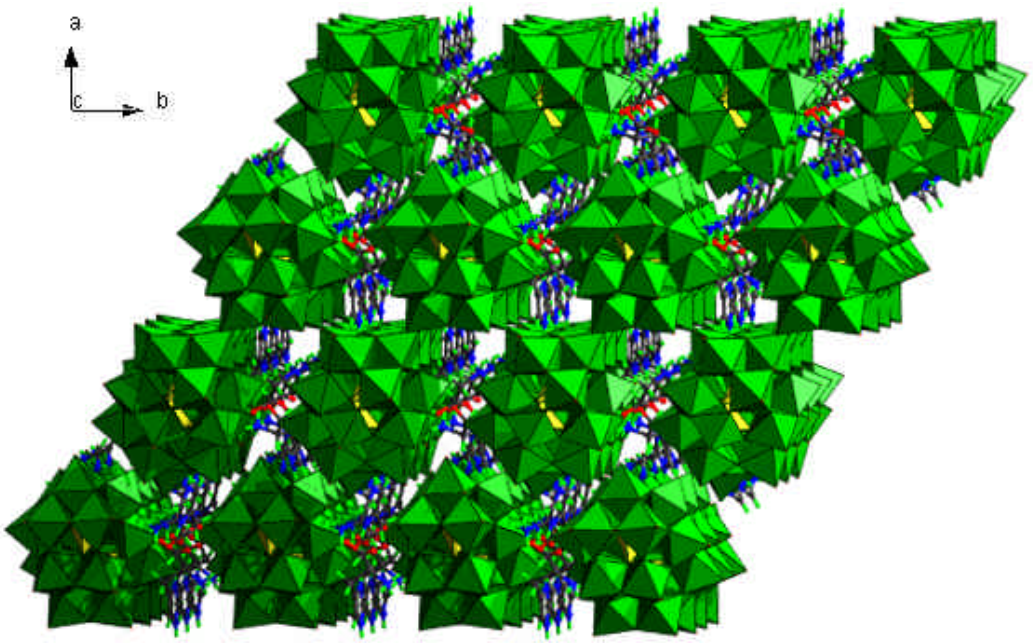

Figure S5 Polyhedral and ball-and-stick representation of the 3D supramolecular structure of **1a** viewed along c axis

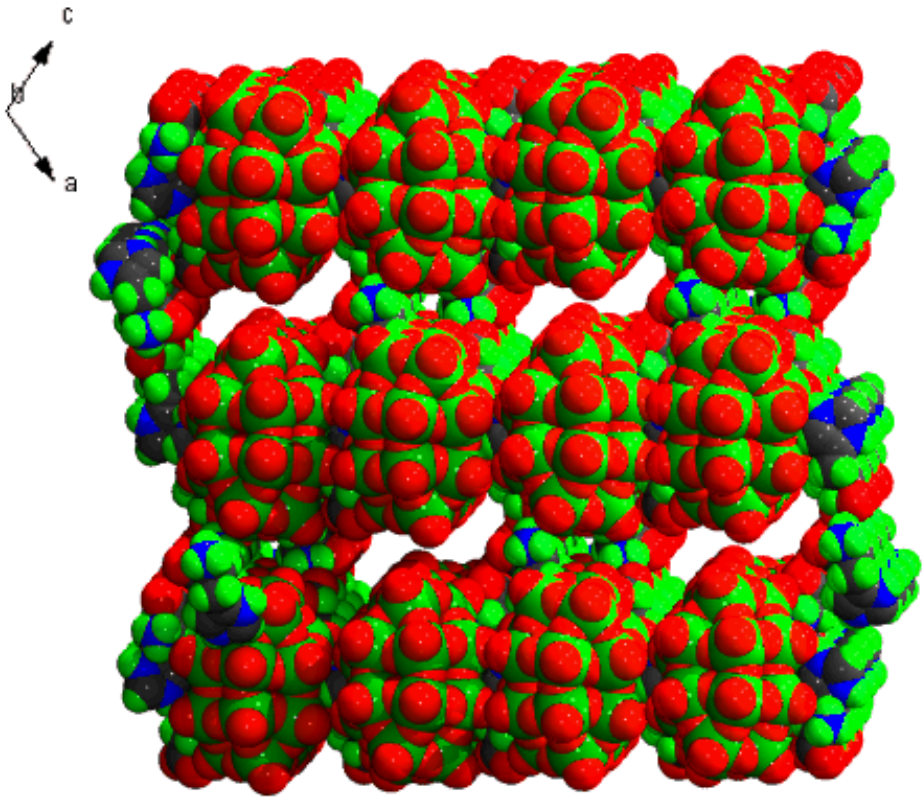

Figure S6 A space-filling diagram representation of 3D supramolecular structure with channels in compound **1a**.

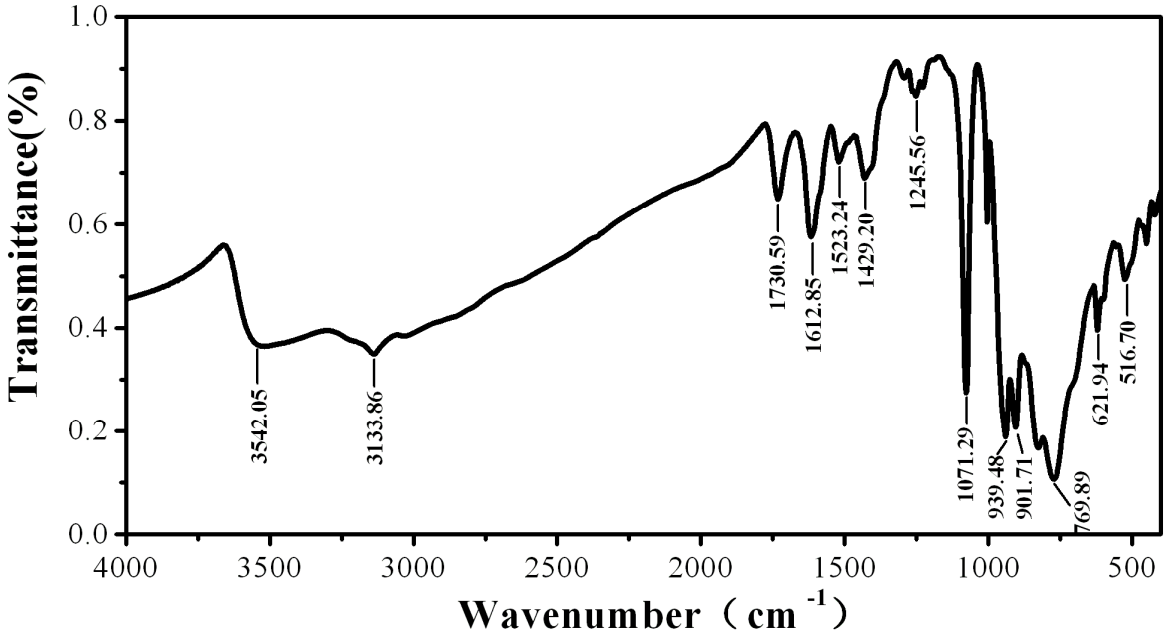

(a)

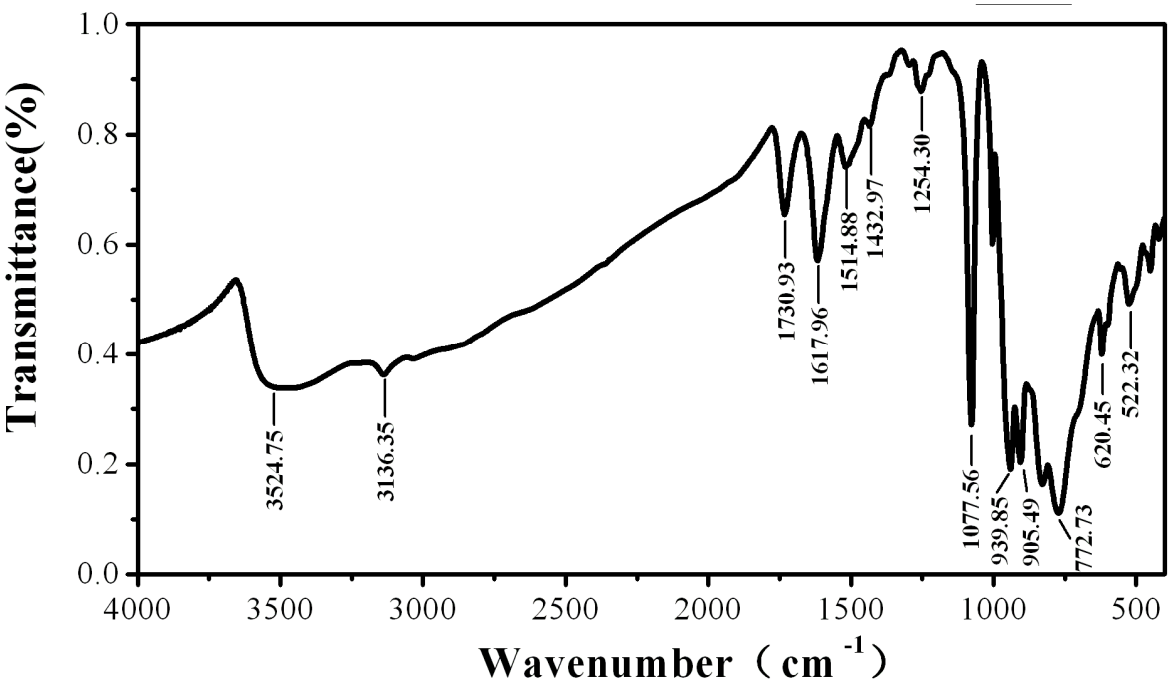

(b)

Figure S7. IR spectrum for compounds **1a** and **1b**

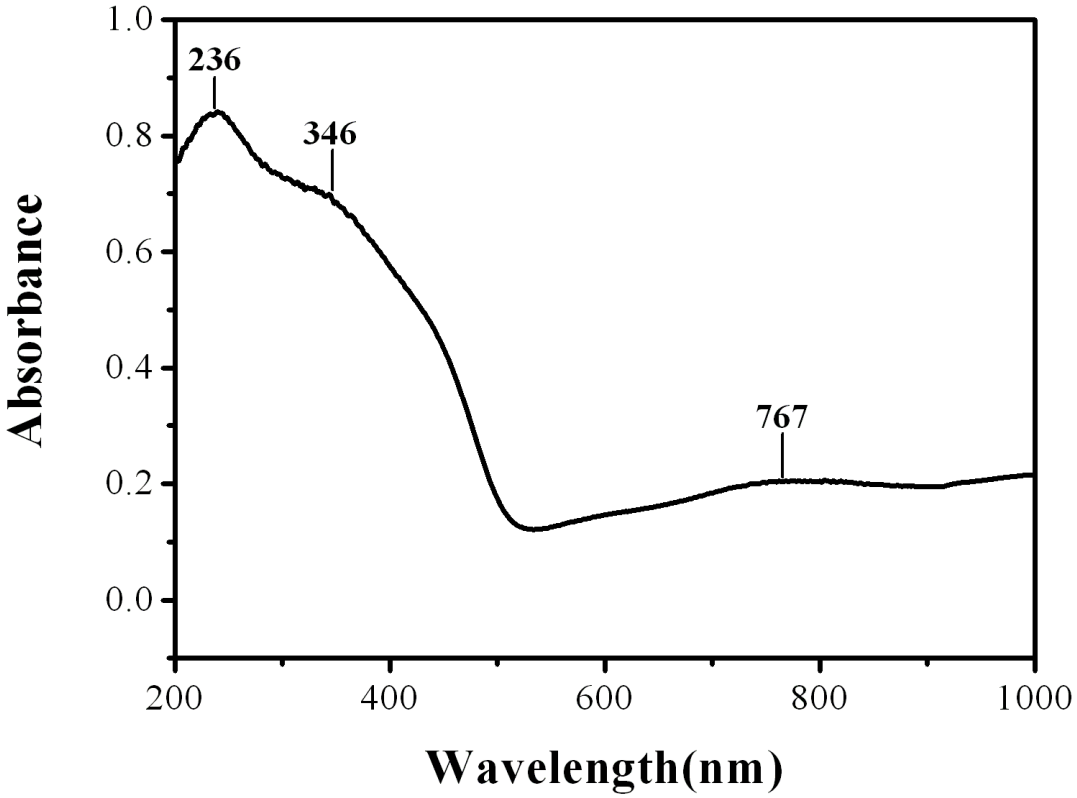

Figure S8. The UV-Vis spectrum for compounds **1a** in the solid state.

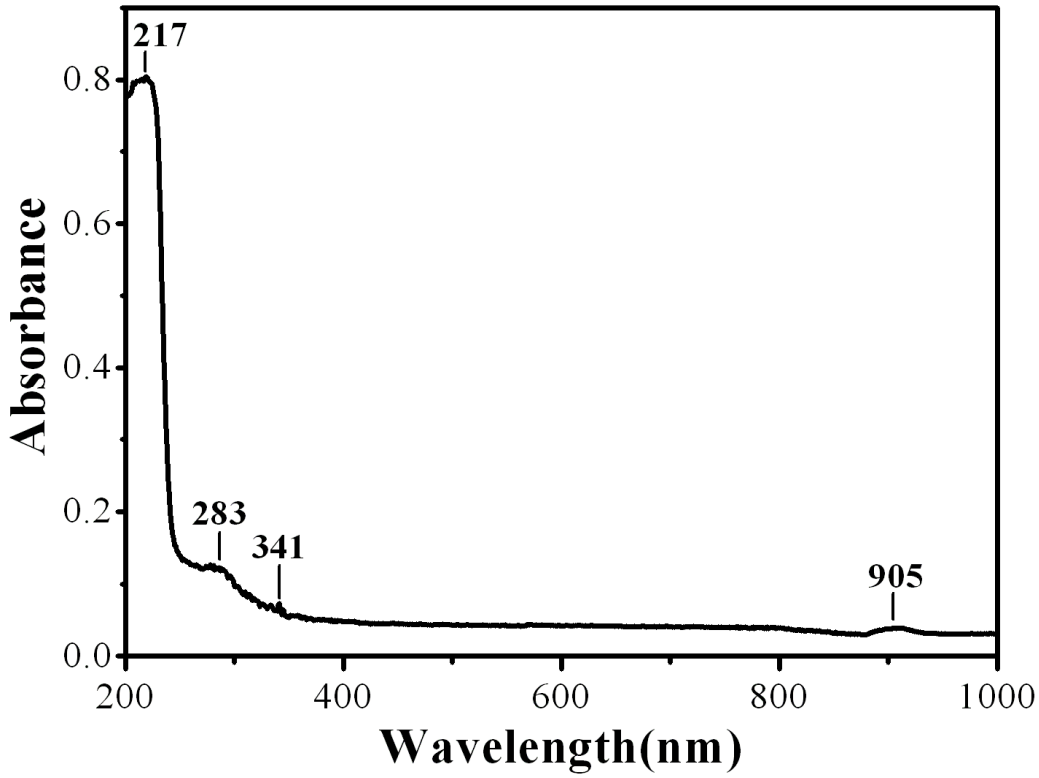

Figure S9. The UV-Vis spectrum for L-histidine in the solid state.

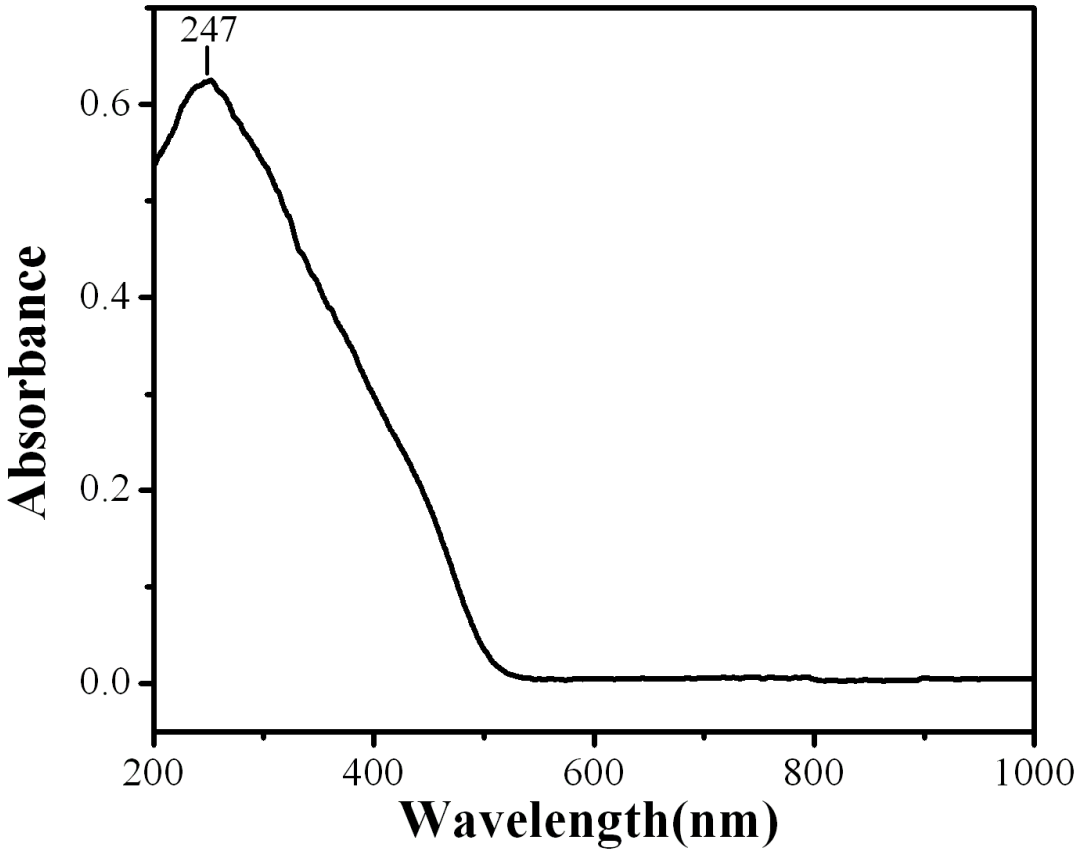

Figure S10. The UV-Vis spectrum for polyoxoanion $[P_2Mo_{18}O_{62}]^{6-}$ in the solid state.

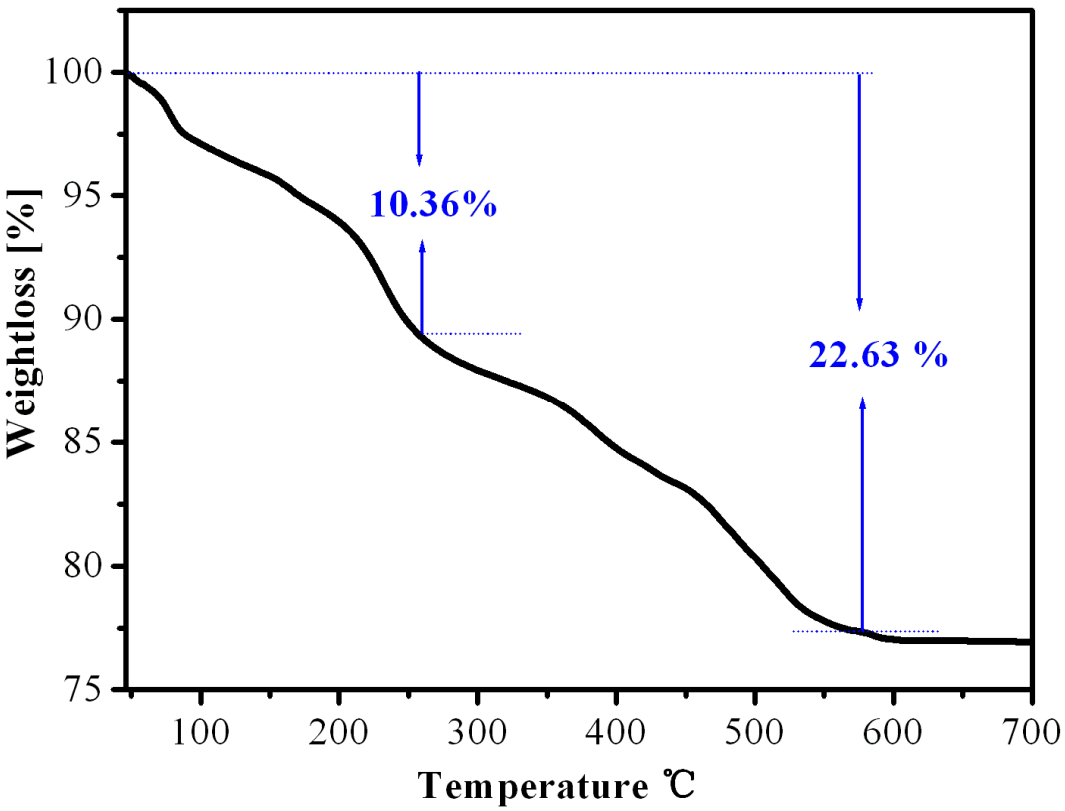

Figure S11. The TG curve of compound **1** exhibits two weight loss stages in the temperature ranges 46-570°C, corresponding to the loss of coordinated water and histidine molecules respectively. The whole weight loss (22.63%) is in good agreement with the calculated value (22.93%).

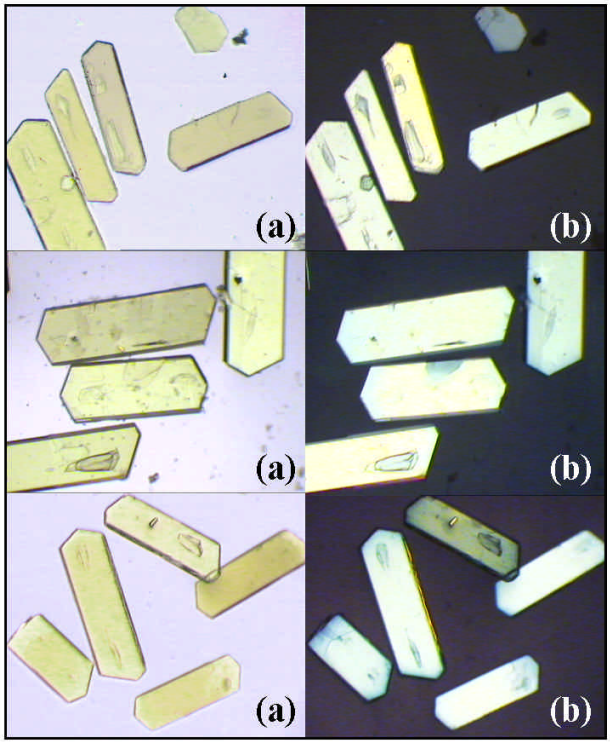

Figure S12. The polarizing optical micrographs of compound **1a**. (a) The bright field images of compound **1a** crystals; (b) The dark field images of compound **1a** crystals.

Table S1 Selected H-bonding for compound **1a** and **1b**

Compound **1a**		Compound **1b**	
O(20)-H(1A)	2.44	O(55)-H(9C)	2.483
H(18A)-O(35)	2.517	O(59)-H(1A)	2.553
O(35)-H(5B)	2.526	H(16A)-O(55)	2.554
O(14)-H(11A)	2.531	O(45)-H(17B)	2.567
O(45)-H(2B)	2.531	H(6A)-O(4)	2.569
O(20)-H(3A)	2.569	O(59)-H(6B)	2.586
H(18A)-O(37)	2.598	O(33)-H(6B)	2.607
O(22)-H(2A)	2.598	O(61)-H(17A)	2.608
O(24)-H(5A)	2.599	O(57)-H(14A)	2.628
H(8B)-O(30)	2.617	H(2A)-O(51)	2.661

O(37)-H(7B)	2.673	O(25)-H(5B)	2.7
O(11)-H(8B)	2.676	O(50)-H(16A)	2.702
O(35)-H(9A)	2.679	O(55)-H(9A)	2.707
O(19)-H(2C)	2.693	O(33)-H(5A)	2.711
O(20)-H(1C)	2.693	H(2A)-O(18)	2.715
O(30)-H(6B)	2.696	O(56)-H(91A)	2.729
H(7A)-O(1)	2.706	O(59)-H(31A)	2.731
O(61)-H(3A)	2.706	H(9B)-O(32)	2.737
O(37)-H(7A)	2.735	H(1A)-O(62)	2.752
H(1B)-O(60)	2.751	O(33)-H(5B)	2.762
O(55)-H(2B)	2.769	O(51)-H(2C)	2.769
H(5B)-O(58)	2.792	O(56)-H(14A)	2.782
H(9B)-O(32)	2.804	O(36)-H(17B)	2.786
O(1)-H(15A)	2.83	O(21)-H(15A)	2.805
O(8)-H(4D)	2.837	H(9C)-O(32)	2.814
O(37)-H(9A)	2.854	O(34)-H(6A)	2.821
O(54)-H(8A)	2.855	O(25)-H(7A)	2.839
O(61)-H(6A)	2.855	O(27)-H(8B)	2.843
O(47)-H(6A)	2.86	O(16)-H(31A)	2.849
O(26)-H(11A)	2.862	O(47)-H(2B)	2.859
O(60)-H(1A)	2.866	O(33)-H(31A)	2.866
H(9A)-O(8)	2.87	O(59)-H(2A)	2.871
H(14A)-O(48)	2.871	H(1A)-O(13)	2.874
O(35)-H(8B)	2.873	H(2B)-O(9)	2.88
O(25)-H(8A)	2.877	O(16)-H(3B)	2.881
O(18)-H(1C)	2.89	O(22)-H(31A)	2.886
H(5A)-O(31)	2.91	H(14A)-O(37)	2.901
O(25)-H(4C)	2.918	O(47)-H(3C)	2.911
H(5B)-O(7)	2.919	H(9A)-O(63)	2.922
O(17)-H(6A)	2.923	O(36)-H(8C)	2.943
O(55)-H(3B)	2.94	H(15A)-O(50)	2.956
H(2C)-O(47)	2.943	H(15A)-O(45)	2.96
O(45)-H(6A)	2.962	H(15A)-O(3)	2.964
H(18A)-O(24)	2.964	H(2C)-O(41)	2.982
O(4)-H(6A)	2.976	H(9B)-O(63)	2.988
O(45)-H(3A)	3.004	O(55)-H(8C)	2.999